Swift Disaster Recovery for Resilient Power Grids: Integration of DERs with Mobile Power Sources

Mostafa Nazemi, *Student Member, IEEE,* Payman Dehghanian, *Member, IEEE*, and Zijiang Yang, *Student Member, IEEE*

***Abstract*—Despite remarkable growth in penetration of renewable energy resources in power grids, most recovery and restoration strategies cannot fully harness the potentials in such resources due to their inherent uncertainty and stochasticity. We propose a resilient disaster recovery scheme to fully unlock the flexibility of the distribution system (DS) through reconfiguration practices and efficient utilization of mobile power sources (MPS) across the system. A novel optimization framework is proposed to model the MPSs dispatch while considering a set of scenarios to capture the uncertainties in distributed energy resources in the system. The optimization model is then convexified equivalently and linearized into a mixed-integer linear programming formulation to reduce the computational complexity and achieve a global optimality. The numerical results verify a notable recovery speed and an improved power system resilience and survivability to severe extremes with devastating consequences.**

***Index Terms*—Distribution systems (DS); high-impact low-probability (HILP) hazards; mobile power sources (MPS); routing and scheduling; dynamic reconfiguration; renewable energy.**

NOMENCLATURE

A. Sets and Indices

$\omega \in \mathbf{\Omega}$	Index/set of scenarios.
$i, j \in \mathbf{B}$	Index/set of network nodes.
$m \in \mathbf{M}$	Index/set of mobile power sources (MPSs).
$t, \tau \in \mathbf{T}$	Index/set of time periods.
$(i, j) \in \mathbf{L}$	Index/set of distribution branches.
$N_{\mathbf{B}}, N_{\mathbf{T}}, N_{\mathbf{L}}$	Number of all nodes, time periods, branches.
$\mathbf{B}^{\text{sub}}$	Set of substation nodes.
$\mathbf{B}_m$	Set of candidate nodes that can be connected to MPS m.
$\mathbf{B}_t^{\text{source}}$	Set of nodes selected to be the source of the fictitious flows at time t.
$\mathbf{L}^{\text{switch}}$	set of branches equipped with remotely-controlled switches.
$\mathbf{L}_t^{\text{damaged}}$	Set of branches that are damaged and have not been repaired at time t.
$\mathbf{G} \in \mathbf{M}$	Set of all mobile emergency generators (MEGs).
$\mathbf{S} \in \mathbf{M}$	Set of all mobile energy storage systems (MESSs).
$\mathbf{V} \in \mathbf{M}$	Set of all mobile electric vehicle (EV) fleets.
$\mathbf{M_i}$	Set of MPSs that can be connected to node i.

B. Parameters and Constants

π_ω	Probability of scenario ω.
υ_i	Priority of the load demanded at node i.
$\ell_{ij,t}$	Binary damage status of branch (i, j) at time t (1 if the branch is not damaged or has been repaired, 0 otherwise).
$\ell^0_{ij,t}$	Binary parameter representing the initial status of branch (i,j) (1 if connected, 0 otherwise).
$p^{\text{fpv}}_{\omega,i,t}$	Forecasted photovoltaic power in scenario ω at node i at time t (kW).
$p^{\text{fw}}_{\omega,i,t}$	Forecasted wind power in scenario ω at node i at time t (kW).
$P^{\text{d}}_{i,t}$	Real power demand of node i at time t (kW).
$Q^{\text{d}}_{i,t}$	Reactive power demand of node i at time t (kVar).
∂_t	Number of microgrids due to the damaged and un-repaired branches at time t.
N_i^{mps}	Number of MPSs that are allowed to be connected to node i.
$T^{\text{travel}}_{m,ij}$	Travel time of MPS m from node i to node j.
Δt	Duration of one time period.
M	A large enough positive number.
$\underline{\text{SoC}}_m$	Minimum state of charge (SoC) of MESS or EV fleet m (kWh).
$\overline{\text{SoC}}_m$	Maximum SoC of the MESS or EV fleet m (kWh).
$\overline{P}^{\text{ch}}_m, \overline{P}^{\text{dch}}_m$	Maximum charging and discharging power of MESS or EV fleet m (kW, kVar).
$\overline{P}_m, \overline{Q}_m$	Maximum real and reactive power output of MPS m (kW, kVar).
$\overline{P}_{ij}, \overline{Q}_{ij}$	Real and reactive power capacity of branch (i, j) (kW, kVar).
r_{ij}, x_{ij}	Resistance and reactance of branch (i, j) (Ω).
$\underline{\text{Vsqr}}_i$	Minimum squared voltage magnitude at node i (kV^2).

M. Nazemi and P. Dehghanian are with the Department of Electrical and Computer Engineering, George Washington University, Washington, DC 20052, USA (e-mails: mostafa_nazemi@gwu.edu; payman@gwu.edu).

Z.Yang is with the China Energy Engineering Group, Guangdong Electric Power Design Institute Co., Ltd, Guangzhou, Guangdong 510663, China (e-mail: yangzijiang5927@163.com).

978-1-7281-2822-1/20/$31.00 ©2020 IEEE

$\overline{\text{Vsqr}}_i$	Maximum squared voltage magnitude at node i (kV^2).
$\eta_m^{\text{ch}}, \eta_m^{\text{dch}}$	Charging and discharging efficiency of MESS or EV fleet m.
P_m^{travel}	Energy Consumption rate of EV fleet m when traveling (kW).
$d_{i,t}^{\text{fic}}$	Fictitious load of node i at time t.

C. Functions and Variables

$pd_{i,t}^s, qd_{i,t}^s$	Real and reactive power demand supplied at node i at time t (kW, kVar).
$pg_{s_i,t}, qg_{s_i,t}$	Real and reactive power at substation at time t (kW, kVar).
$pf_{ij,t}, qf_{ij,t}$	Real and reactive power flow on branch (i,j) at time t (kW, kVar).
$\text{SoC}_{m,t}$	SoC of MESS or EV fleet m at time t (kWh).
$p_{m,t}^{\text{ch}}, p_{m,t}^{\text{dch}}$	Charging and discharging power of MESS or EV fleet m at time t (kW).
$p_{m,t}, q_{m,t}$	Real and reactive power output of MPS m at time t (kW, kVar).
$P_{i,t}^{\text{mps}}, Q_{i,t}^{\text{mps}}$	Real and reactive power output of MPS at node i (kW, kVar).
$V_{i,t}^{\text{sqr}}$	Squared voltage magnitude at node i at time t (kV^2).
$fl_{ij,t}$	Fictitious flow on branch (i,j) at time t.
$fg_{i,t}$	Fictitious supply at source node i at time t.
$p_{i,t}^{pv}$	Stochastic realization of active photovoltaic power at node i and time t.
$p_{i,t}^{w}$	Stochastic realization of active wind power at node i and time t.
$q_{i,t}^{pv}$	Stochastic realization of reactive photovoltaic power at node i and time t.
$q_{i,t}^{w}$	Stochastic realization of reactive wind power at node i and time t.

D. Binary Variables

$\alpha_{ij,t}$	Connection status of branch (i,j) at time t (1 if the branch is connected, 0 otherwise).
$c_{m,t}, d_{m,t}$	Charging and discharging status of MESS or EV fleet m at time t (1 if it is charging or discharging; 0 otherwise).
$\varphi_{m,t}$	Traveling status of MPS m at time t (1 if the MPS is traveling; 0 otherwise).
$\mu_{m,i,t}$	Connection status of MPS m to node i at time t (1 if connected; 0 otherwise).

I. Introduction

Occurrence of natural disasters and cyber attacks has been observed to be on the rise over past decades [1], [2]. This, therefore, demands for developing effective mechanisms that ensure a continuous and resilient supply of electricity to the end customers [3]–[8].

Power distribution system (DS) resilience to disastrous events can be boosted by holistic planning, operation, and control of microgrids by which critical loads can be supplied during emergencies [9], [10]. Grid-support mobile power sources (MPSs) including electric vehicles (EVs), truck-mounted mobile energy storage systems (MESSs), and mobile emergency generators (MEGs) offer spatial flexibility advantages to elevate the DS resilience primarily driven by harnessing their mobility [11]. If MPSs are effectively routed and scheduled through a comprehensive optimization model, they can be considered as backup power sources to prevent outages to some extent even if the system loses access to the main grid [12], [13]. Following a high-impact low-probability (HILP) hazard, DS network reconfiguration also plays a significant role in rerouting and delivering the power from MPSs to critical loads by switching some branches on and off [14]–[17]. The distribution branches can be equipped with remotely-controlled switches (RCS) which can change the system configuration by changing the boundaries of different isolated microgrids following a HILP event. DS configuration may change due to the unavailability of distribution lines and other elements. Hence, prompt restoration of critical loads highly depends on (i) the operability of a to-be-repaired distribution branch, (ii) the availability of an MPS at a specific node, and (iii) the availability of distributed energy resources (DERs).

The increasing proliferation of DERs such as solar and wind resources has been resulted in more flexibility and potentials for swift disaster recovery; however, the uncertain and intermittent renewable generation portfolios have introduced significant challenges to today's grid operation and control paradigms. Such uncertainties, if not properly modeled and accounted for, may change the underlying principles of optimization mechanisms and, at times, may render this potential unlocked [18]. In this paper, a mixed-integer nonlinear programming (MINLP) model is proposed for routing and scheduling of MPSs coordinated with the DS reconfiguration to improve resilience against HILP events. The existing uncertainties in the DS, i.e., solar and wind resources, are incorporated into the optimization model by considering a suite of scenarios. The MINLP model is further linearized into a mixed-integer linear programming (MILP) model to effectively address the computation complexity and then solved by the-off-shelf commercial solvers. Multiple types of MPSs, e.g., MEGs, MESSs and EVs, are dispatched considering the repair schedules of the damaged branches to facilitate the DS restoration process and to realize enhanced resilience.

The rest of this paper is organized as follows. The proposed optimization formulation is presented in Section II while the applied linearization technique is explained in Section III. Numerical results and discussion are provided in Section IV and Section V concludes the paper.

II. Problem Formulation

In this section and inspired by [19], the optimization formulations for routing and scheduling of MPS considering the stochasticity of renewable resources is presented as follows.

$$\max \left(\sum_{t\in\mathbf{T}}\sum_{i\in\mathbf{B}} \upsilon_i \cdot pd^s_{i,t} + \sum_{t\in\mathbf{T}}\sum_{i\in\mathbf{B}} (p^{pv}_{i,t} + p^{w}_{i,t}) \right) \quad (1)$$

$$\sum_{i\in\mathbf{B}_m} \mu_{m,i,t} \le 1, \forall m \in \mathbf{M}, \forall t \in \mathbf{T} \quad (2)$$

$$\sum_{m\in\mathbf{M}_i} \mu_{m,i,t} \le N^{\text{mps}}_i, \forall i \in \bigcup_{m\in\mathbf{M}} \mathbf{B}_m, \forall t \in \mathbf{T} \quad (3)$$

$$\varphi_{m,t} = 1 - \sum_{i\in\mathbf{B}_m} \mu_{m,i,t}, \forall m \in \mathbf{M}, \forall t \in \mathbf{T} \quad (4)$$

$$\begin{aligned} &\mu_{m,i,t+\tau} + \mu_{m,j,t} \le 1, \\ &\forall m \in \mathbf{M},\ \forall i,j \in \mathbf{B}_m,\ \forall \tau \le T^{\text{travel}}_{m,ij},\ \forall t+\tau \le N_{\mathbf{T}} \end{aligned} \quad (5)$$

$$\begin{aligned} \text{SoC}_{m,t} = \text{SoC}_{m,t-1} + (\eta^{\text{ch}}_m \cdot p^{\text{ch}}_{m,t} - p^{\text{dch}}_{m,t}/\eta^{\text{dch}}_m) \cdot \Delta t, \\ \forall m \in \mathbf{S},\ \forall t \ge 1 \end{aligned} \quad (6)$$

$$\begin{aligned} \text{SoC}_{m,t} = \text{SoC}_{m,t-1} + (\eta^{\text{ch}}_m \cdot p^{\text{ch}}_{m,t} - p^{\text{dch}}_{m,t}/\eta^{\text{dch}}_m - \\ \varphi_{m,t} \cdot P^{\text{travel}}_m) \cdot \Delta t, \qquad \forall m \in \mathbf{V},\ \forall t \ge 1 \end{aligned} \quad (7)$$

$$\underline{\text{SoC}}_m \le \text{SoC}_{m,t} \le \overline{\text{SoC}}_m, \forall m \in \{\mathbf{S},\mathbf{V}\}, \forall t \in \mathbf{T} \quad (8)$$

$$0 \le p^{\text{ch}}_{m,t} \le c_{m,t} \cdot \overline{P}^{\text{ch}}_m, \forall m \in \{\mathbf{S},\mathbf{V}\}, \forall t \in \mathbf{T} \quad (9)$$

$$0 \le p^{\text{dch}}_{m,t} \le d_{m,t} \cdot \overline{P}^{\text{dch}}_m, \forall m \in \{\mathbf{S},\mathbf{V}\}, \forall t \in \mathbf{T} \quad (10)$$

$$c_{m,t} + d_{m,t} \le \sum_{i\in\mathbf{B}_m} \mu_{m,i,t}, \forall m \in \{\mathbf{S},\mathbf{V}\}, \forall t \in \mathbf{T} \quad (11)$$

$$0 \le p_{m,t} \le \sum_{i\in\mathbf{B}_m} \mu_{m,i,t} \cdot \overline{P}_m, \forall m \in \mathbf{G}, \forall t \in \mathbf{T} \quad (12)$$

$$0 \le q_{m,t} \le \sum_{i\in\mathbf{B}_m} \mu_{m,i,t} \cdot \overline{Q}_m, \forall m \in \mathbf{G}, \forall t \in \mathbf{T} \quad (13)$$

$$\sum_{(i,j)\in\mathbf{L}} \alpha_{ij,t} = N_{\mathbf{B}} - \partial_t, \forall t \in \mathbf{T} \quad (14)$$

$$\sum_{(j,i)\in\mathbf{L}} fl_{ji,t} - \sum_{(i,j)\in\mathbf{L}} fl_{ij,t} = d^{\text{fic}}_{i,t}, \forall i \in \mathbf{B}\backslash\mathbf{B}^{\text{source}}_t, \forall t \in \mathbf{T} \quad (15)$$

$$\sum_{(i,j)\in\mathbf{L}} fl_{ij,t} - \sum_{(j,i)\in\mathbf{L}} fl_{ji,t} = fg_{i,t}, \forall i \in \mathbf{B}^{\text{source}}_t, \forall t \in \mathbf{T} \quad (16)$$

$$-\alpha_{ij,t} \cdot M \le fl_{ij,t} \le \alpha_{ij,t} \cdot M, \forall (i,j) \in \mathbf{L}, \forall t \in \mathbf{T} \quad (17)$$

$$\alpha_{ij,t} \le \ell_{ij,t}, \forall (i,j) \in \mathbf{L}, \forall t \in \mathbf{T} \quad (18)$$

$$\alpha_{ij,t} = \ell^0_{ij,t}, \forall (i,j) \in \mathbf{L}\backslash\{\mathbf{L}^{\text{damaged}}_t, \mathbf{L}^{\text{switch}}\}, \forall t \in \mathbf{T} \quad (19)$$

$$\begin{aligned} P^{\text{mps}}_{i,t} = &\sum_{m\in\mathbf{M}_i\cap\{\mathbf{S},\mathbf{V}\}} \mu_{m,i,t} \cdot p^{\text{dch}}_{m,t} - \sum_{m\in\mathbf{M}_i\cap\{\mathbf{S},\mathbf{V}\}} \mu_{m,i,t} \cdot p^{\text{ch}}_{m,t} \\ &+ \sum_{m\in\mathbf{M}_i\cap\mathbf{G}} \mu_{m,i,t} \cdot p_{m,t}, \quad \forall i \in \bigcup_{m\in\mathbf{M}} \mathbf{B}_m, \forall t \in \mathbf{T} \end{aligned} \quad (20)$$

$$Q^{\text{mps}}_{i,t} = \sum_{m\in\mathbf{M}_i} \mu_{m,i,t} \cdot q_{m,t}, \quad \forall i \in \bigcup_{m\in\mathbf{M}} \mathbf{B}_m, \forall t \in \mathbf{T} \quad (21)$$

$$P^{\text{mps}}_{i,t} = Q^{\text{mps}}_{i,t} = 0, \quad \forall i \in \mathbf{B}\backslash \bigcup_{m\in\mathbf{M}} \mathbf{B}_m, \forall t \in \mathbf{T} \quad (22)$$

$$\begin{aligned} \sum_{(j,i)\in\mathbf{L}} pf_{ji,t} - \sum_{(i,j)\in\mathbf{L}} pf_{ij,t} = pd^s_{i,t} - pg_{s_i,t} \\ - P^{\text{mps}}_{i,t} - p^{\text{pv}}_{i,t} - p^{\text{w}}_{i,t}, \quad \forall i \in \mathbf{B}, \forall t \in \mathbf{T} \end{aligned} \quad (23)$$

$$\begin{aligned} \sum_{(j,i)\in\mathbf{L}} qf_{ji,t} - \sum_{(i,j)\in\mathbf{L}} qf_{ij,t} = qd^s_{i,t} - qg_{s_i,t} \\ - Q^{\text{mps}}_{i,t} - q^{\text{pv}}_{i,t} - q^{\text{w}}_{i,t}, \quad \forall i \in \mathbf{B}, \forall t \in \mathbf{T} \end{aligned} \quad (24)$$

$$0 \le pd^s_{i,t} \le P^{\text{d}}_{i,t}, \forall i \in \mathbf{B},\ \forall t \in \mathbf{T} \quad (25)$$

$$0 \le p^{\text{pv}}_{i,t} \le \sum_{\omega\in\mathbf{\Omega}} \pi_\omega . p^{\text{fpv}}_{\omega,i,t},\ \forall i \in \mathbf{B},\ \forall t \in \mathbf{T} \quad (26)$$

$$0 \le p^{\text{w}}_{i,t} \le \sum_{\omega\in\mathbf{\Omega}} \pi_\omega . p^{\text{fw}}_{\omega,i,t},\ \forall i \in \mathbf{B},\ \forall t \in \mathbf{T} \quad (27)$$

$$q^{\text{pv}}_{i,t} = (Q^{\text{d}}_{i,t}/P^{\text{d}}_{i,t}) \cdot p^{\text{pv}}_{i,t},\ \forall i \in \mathbf{B},\ \forall t \in \mathbf{T} \quad (28)$$

$$q^{\text{w}}_{i,t} = (Q^{\text{d}}_{i,t}/P^{\text{d}}_{i,t}) \cdot p^{\text{w}}_{i,t},\ \forall i \in \mathbf{B},\ \forall t \in \mathbf{T} \quad (29)$$

$$pd^s_{i,t-1}/P^{\text{d}}_{i,t-1} \le pd^s_{i,t}/P^{\text{d}}_{i,t}, \forall i \in \mathbf{B},\ \forall t \ge 1 \quad (30)$$

$$qd^s_{i,t} = (Q^{\text{d}}_{i,t}/P^{\text{d}}_{i,t}) \cdot pd^s_{i,t}, \forall i \in \mathbf{B},\ \forall t \in \mathbf{T} \quad (31)$$

$$-\alpha_{ij,t} \cdot \overline{P}_{ij} \le pf_{ij,t} \le \alpha_{ij,t} \cdot \overline{P}_{ij}, \forall (i,j) \in \mathbf{L}, \forall t \in \mathbf{T} \quad (32)$$

$$-\alpha_{ij,t} \cdot \overline{Q}_{ij} \le qf_{ij,t} \le \alpha_{ij,t} \cdot \overline{Q}_{ij}, \forall (i,j) \in \mathbf{L}, \forall t \in \mathbf{T} \quad (33)$$

$$\begin{aligned} V^{\text{sqr}}_{i,t} - V^{\text{sqr}}_{j,t} \le &(1-\alpha_{ij,t}) \cdot M + 2 \cdot (r_{ij} \cdot pf_{ij,t} + \\ &x_{ij} \cdot qf_{ij,t}), \quad \forall (i,j) \in \mathbf{L}, \forall t \in \mathbf{T} \end{aligned} \quad (34)$$

$$\begin{aligned} V^{\text{sqr}}_{i,t} - V^{\text{sqr}}_{j,t} \ge &(\alpha_{ij,t} - 1) \cdot M + 2 \cdot (r_{ij} \cdot pf_{ij,t} + \\ &x_{ij} \cdot qf_{ij,t}), \quad \forall (i,j) \in \mathbf{L}, \forall t \in \mathbf{T} \end{aligned} \quad (35)$$

$$\underline{\text{Vsqr}}_i \le V^{\text{sqr}}_{i,t} \le \overline{\text{Vsqr}}_i, \forall i \in \mathbf{B}, \forall t \in \mathbf{T} \quad (36)$$

Motivated by [11], the objective function (1) includes two terms as follows: the first term is the total supplied load considering the priority of the load points over the entire time period; and the second term is to maximize the utilization of renewables, i.e., solar and wind energy. A number of constraints need to be taken into account for the DS restoration problem as follows.

1) MPS Connection Constraints: Following a HILP event, the MPSs will quickly travel and get connected in the isolated microgrids to supply the demanded power. At each time period, the MPS can be connected to at most one pre-determined candidate node, as enforced in (2). Constraint (3) indicates that the allowed number of MPSs connected to a node is limited to the stations' capacity at each candidate node. Constraint (4) states that the MPSs cannot travel to other nodes when connected to a candidate node.

2) MPS Routing Constraints: constraint (5) ensures that the MPSs transportation among different DS nodes satisfies the required travel time.

3) MPS Power Scheduling Constraints: It is assumed that the truck-mounted MESS and MEG can be refueled with tanker trunk for transportation during the restoration process [20], while EVs consume their own electric energy to transfer from one to another node. The change in the state of charge (SoC) of MESSs over time is determined by their charging and

discharging behaviors, as represented in (6) while the SoC of EVs is determined by their charging and discharging as well as travel behaviors (7). Constraint (8) restricts the range of SoC of MESS and EV over all time periods. Constraint (9) and (10) respectively impose the range of charging and discharging power for MESS and EV according to the corresponding rated power. The charging and discharging power are both enforced to be zero when MESS and EV are not connected to the DS. Charging and discharging of MESS and EV are mutually exclusive over all time periods, as represented in (11) which indicates that the MPS disconnected from DS can neither charge nor discharge. Constraint (12) and (13) set the range of real and reactive power output of MEG according to its rated power, respectively, and enforce MEG to have zero real and reactive output when it is disconnected from DS.

4) DS Radiality Constraints: Constraints (14)-(17) ensure that the DS remains radial over all time periods. For DS radiality, there are two conditions which need to be satisfied: (i) at each PI, the number of connected branches is equal to the total number of nodes in the PI-1; (ii) all load points are connected to a determined source node in each PI. The first condition is satisfied in constraint (14). In each PI, one node is considered as a fictitious source node and the remaining nodes are fictitious load points. The fictitious source node and fictitious load node are the source and the destination of fictitious power flow, respectively. The amount of the fictitious flow into a load node $d_{i,t}^{\text{fic}}$ is set as 1 at all nodes. The second condition is satisfied in constraint (15)-(17) that enforce each load node to receive one unit of the fictitious flow from the fictitious source node at each PI. Constraints (15)-(16) ensure the fictitious flow balance for the fictitious load and source nodes, respectively. Constraint (17) enforces the fictitious flow to be zero in open branches. The large enough positive number M relaxes this constraint when some branches are open (See [21] for additional details on the fictitious network and radiality conditions).

5) Branch Status Constraints: According to (18), the damaged branch must be open if it has not yet been repaired at time t. Constraint (19) states that the undamaged branches without RCS remain in their initial status over all time periods.

6) MPS Output Power Constraints: Constraints (20)-(21) indicate that the real or reactive power injection or extraction at a candidate node for MPS siting is equal to the sum of the real or reactive power output of the MPSs. The non-MPS nodes are attributed zero real and reactive power from MPSs as expressed in (22).

7) Power Balance Constraints: Constraints (23)-(24) describe the real and reactive power balance conditions at all nodes, respectively. The range of the demanded load to be supplied is bounded in constraint (25). Constraints (26)-(27) reflect the relation of stochastic realization of solar and wind energies with the forecasted values in each scenario. A thousand number of scenarios are considered here to capture the uncertainties in the forecasted values at each time period. Constraints (28)-(29) indicate the relation of the scheduled reactive and active solar and wind power. Constraint (30) enforces the recovery rate of the supplied loads not to decrease. The power factor of the demand is assumed to be fixed in (31). The real and reactive power flows in the online branches are respectively limited by their real and reactive power capacities in (32)-(33). Constraints (32)-(33) also enforce the real and reactive power flow in open branches to be zero.

8) Power Flow Constraints: Constraint (34) and (35) represent the power flow equation in which the M value is a relaxation parameter [22]. Constraint (36) states the boundary for the voltage magnitudes.

III. Linearization Technique

The proposed optimization model is a non-convex mixed-integer non-linear programming (MINLP) model due to constraints (20) and (21). According to [23], a linearization technique is used in this paper as illustrated below:

$$0 \leq P_{m,i,t}^{\text{dch}} \leq \mu_{m,i,t} \cdot \overline{P}_{m}^{\text{dch}} \tag{37}$$

$$p_{m,t}^{\text{dch}} + (\mu_{m,i,t} - 1) \cdot \overline{P}_{m}^{\text{dch}} \leq P_{m,i,t}^{\text{dch}} \leq p_{m,t}^{\text{dch}} \tag{38}$$

$$0 \leq P_{m,i,t}^{\text{ch}} \leq \mu_{m,i,t} \cdot \overline{P}_{m}^{\text{ch}} \tag{39}$$

$$p_{m,t}^{\text{ch}} + (\mu_{m,i,t} - 1) \cdot \overline{P}_{m}^{\text{ch}} \leq P_{m,i,t}^{\text{ch}} \leq p_{m,t}^{\text{ch}} \tag{40}$$

$$0 \leq P_{m,t} \leq \mu_{m,i,t} \cdot \overline{P}_{m} \tag{41}$$

$$p_{m,t} + (\mu_{m,i,t} - 1) \cdot \overline{P}_{m} \leq P_{m,i,t} \leq p_{m,t} \tag{42}$$

$$0 \leq Q_{m,t} \leq \mu_{m,i,t} \cdot \overline{Q}_{m} \tag{43}$$

$$q_{m,t} + (\mu_{m,i,t} - 1) \cdot \overline{Q}_{m} \leq Q_{m,i,t} \leq q_{m,t} \tag{44}$$

For instance, if $\mu_{m,i,t} = 1$, then we have $P_{m,i,t}^{\text{dch}} = p_{m,t}^{\text{dch}}$; if $\mu_{m,i,t} = 0$, then $P_{m,i,t}^{\text{dch}} = 0$. By doing so, the MINLP formulation is linearized into a mixed-integer linear programming (MILP) problem which can be solved by the available off-the-shelf solvers.

IV. Numerical Results and Discussions

In this section, the proposed uncertainty-aware integrated routing and scheduling of MPS with DS reconfiguration is applied to the IEEE 33-node test system to verify the effectiveness of the proposed scheme. All simulations have been conducted on a PC with an Intel Xeon E5-2620 v2 processor and 16 GB of memory using CPLEX 12.5.1.

We assume 9 branches (out of the 37 branches) in the network are unavailable following an adverse HILP event. It is also assumed that 3 stations are available in the DS to connect the MEG and MESS and there are 3 EV stations for charging and discharging of EVs. Moreover, we assume that 3 MPSs are available in the restoration process: one electric bus considered as EV with 150 kW/150 kWh capacity and 0.25 kWh/km energy consumption rate, one MESS with 500 kW/776 kWh capacity, and one MEG with 800kW/600 kVar capacity [13], [24]–[27]. The priority factor of demanded loads is randomly generated between 0 and 10, lying within or lower than the typical value of lost load (VOLL) of different customers [4], [28]. Some other data can be found in [22]. The allocations of 8 RCS, solar panel, and wind turbine are demonstrated in Fig. 1. The total time period is considered $T = 24$, where each time period is Δt=0.5h. All the MPSs are located at the substation node at $t = 1$ and the initial SoC of EV and MESS are considered fully charged. In this paper, 1000 scenarios with

the same probability (π) for each time period are considered to capture the uncertainties in the forecasted values of solar and wind energies. The repair schedule for damaged branches is tabulated in Table I.

According to Table II, tie lines 9-15, 12-22, 18-33, and 25-29 which are normally open (i.e., offline) should be closed (i.e., online) for some time periods in order to change the DS topology and facilitate the routing of MPSs. Note that branch 14-15 and 28-29 are already online during the normal operating conditions, while branches 9-10 and 30-31 are offline due to post-event damages. At t=4∼5, branch 19-20 has been repaired by repair crews; EV 1, MESS 1 and MEG 1 are connected to node 33 and 15, and 29 respectively, to form microgrid 1, 2, and 3. The SoC of EV, and MESS and the real power output of MEG at different time periods is depicted in Fig. 2. As it can be seen, during the first time periods of restoration, all MPS contribute to restore power outages while after $t = 6$ the MESS stops discharging until $t = 21$ when MEG's power output is zero. At t=7, EV 1 starts supplying power while branch 12-22 is open to ensure the DS radial topology since branches 8-9 and 9-10 are repaired and connected back at t=6 and t=7, respectively. At t=9, branch 9-15 is open to ensure the DS radial topology since branch 12-13 is repaired and connected back. At t=13, the branch 16-17 has been repaired; hence, nodes 17, 18, and 33 are re-connected to the substation node and the isolated microgrid is merged with the main grid. EV 1 should travel to node 5 in order to be charged since its SoC is reaching the minimum threshold. At t=18∼19, branch 30-31 has been repaired when EV 1 returns to node 33 and continues supplying the neighbour load points as they have not been yet fully restored—due to the distribution lines capacity limits. Moreover, all load points across the studied DS, except node 24, are supplied with the energy conjointly provided by the main grid and the MPSs at t=18∼19. At t=20, branch 27-28 is repaired and re-energized; thus, branch 18-33 is open to ensure the DS radial topology. At t=22, branch 24-25 is repaired, the DS is fully restored by the main grid substation and all the grid-support MPS resources even though branch 23-24 is not yet repaired.

The forecasted solar energy through 1000 scenarios with the same probability are depicted in Fig. 3. The voltage profile in each time period is depicted in Fig. 4. As it presents, the voltage magnitudes are within the desired limits (0.95-1.05 p.u.) for all nodes in all time slots. The optimized realization of solar and wind during the entire restoration horizon is illustrated in Fig. 5. Utilizing the MPSs conjointly with harnessing the stochastic renewable energies as well as DS dynamic reconfiguration have effectively ensured a swift response and recovery, thereby realizing an enhanced operational resilience against HILP events.

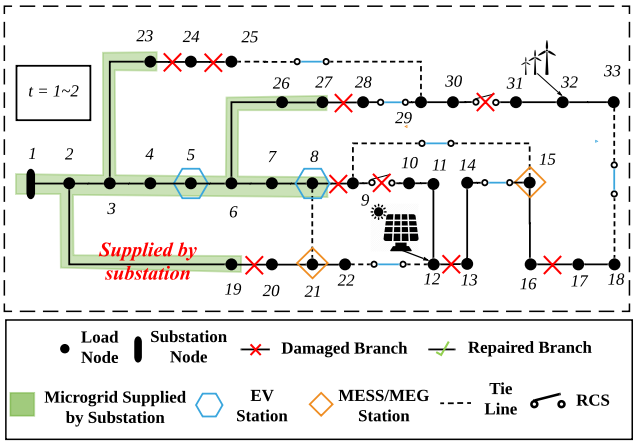

Fig. 1. IEEE 33-node test system split into different microgrids.

TABLE I
TIME SEQUENCE OF REPAIRS FOR DAMAGED BRANCHES

Time Period (t)	3	6	7	9	13
Repaired Branch	19-20	8-9	9-10	12-13	16-17
Time Period (t)	16	20	22	24	
Repaired Branch	30-31	27-28	24-25	23-24	

TABLE II
DYNAMIC NETWORK RECONFIGURATION OF THE DS

Time Period (t)	t=1∼6	t=7∼8	t=9∼19	t=20∼23	t=24
Branch 9-15	Close		Open		
Branch 12-22	Close	Open			
Branch 18-33	Close			Open	
Branch 25-29	Close				Open

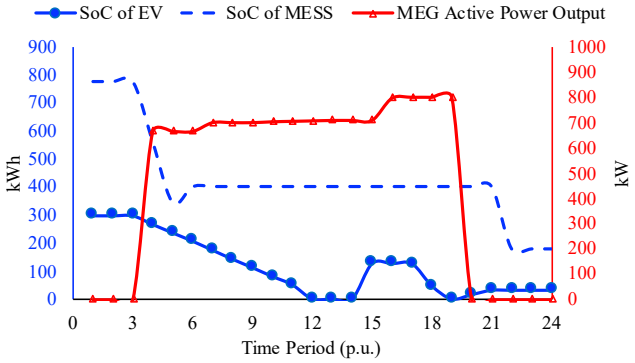

Fig. 2. SoC of EV, MESS, and real power output of MEG in each time period.

V. CONCLUSION

To elevate the resilience and survivability of DS in face of HILP hazards, an optimization model for disaster recovery is proposed in this paper in which MPS dispatch and dynamic network reconfiguration are jointly cooperated with renewable energies. A MINLP optimization model involving a set of thousand scenarios is suggested, linearized, and reformulated to a MILP model so as to realize the DS service restoration. Harnessing the full potentials in renewable energies and capturing the corresponding uncertainties, numerical results revealed the effectiveness of the proposed recovery and restoration strategy.

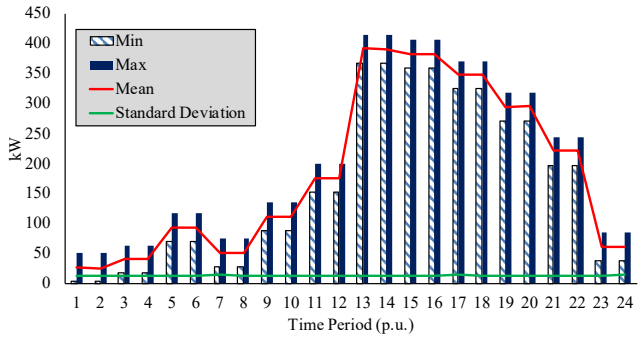

Fig. 3. Solar prediction in 1000 scenarios at each time period.

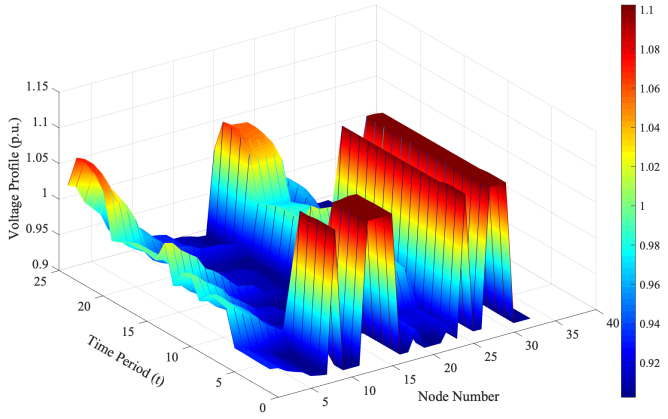

Fig. 4. Voltage profile at each time period.

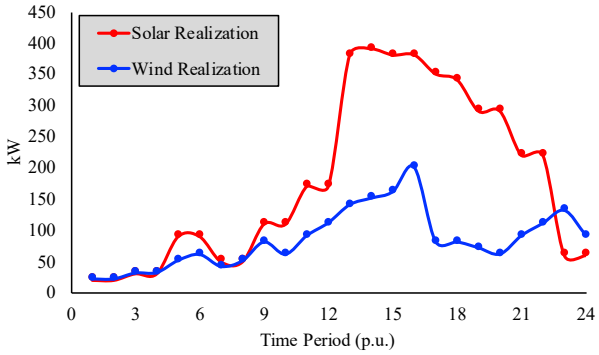

Fig. 5. Stochastic realization of solar and wind energy in the DS.

REFERENCES

[1] P. Dehghanian, B. Zhang, T. Dokic, and M. Kezunovic, "Predictive risk analytics for weather-resilient operation of electric power systems," *IEEE Trans. on Sust. Energy*, vol. 10, no. 1, pp. 3–15, 2019.

[2] P. Dehghanian, S. Aslan, and P. Dehghanian, "Maintaining electric system safety through an enhanced network resilience," *IEEE Transactions on Industry Applications*, vol. 54, no. 5, pp. 4927–4937, 2018.

[3] W. House, "Economic benefits of increasing electric grid resilience to weather outages," *Washington, DC: Exec. Office of the President*, 2013.

[4] M. Nazemi and P. Dehghanian, "Seismic-resilient bulk power grids: Hazard characterization, modeling, and mitigation," *IEEE Transactions on Engineering Management*, 2019.

[5] J. Wang, W. Zuo, L. Rhode-Barbarigos, X. Lu, J. Wang, and Y. Lin, "Literature review on modeling and simulation of energy infrastructures from a resilience perspective," *Reliability Engineering & System Safety*, vol. 183, pp. 360–373, 2019.

[6] M. Nazemi, M. Moeini-Aghtaie, M. Fotuhi-Firuzabad, and P. Dehghanian, "Energy storage planning for enhanced resilience of power distribution networks against earthquakes," *IEEE Transactions on Sustainable Energy*, vol. 11, no. 2, pp. 795–806, 2020.

[7] J. Su, P. Dehghanian, M. Nazemi, and B. Wang, "Distributed wind power resources for enhanced power grid resilience," in *2019 North American Power Symposium (NAPS)*, pp. 1–6, 2019.

[8] S. Wang, P. Dehghanian, M. Alhazmi, and M. Nazemi, "Advanced control solutions for enhanced resilience of modern power-electronic-interfaced distribution systems," *Journal of Modern Power Systems and Clean Energy*, vol. 7, no. 4, pp. 716–730, 2019.

[9] J. Lai, X. Lu, F. Wang, P. Dehghanian, and R. Tang, "Broadcast gossip algorithms for distributed peer-to-peer control in ac microgrids," *IEEE Transactions on Industry Applications*, 2019.

[10] Y. Tan, F. Qiu, A. K. Das, D. S. Kirschen, P. Arabshahi, and J. Wang, "Scheduling post-disaster repairs in electricity distribution networks," *IEEE Trans. on Power Syst.*, vol. 34, no. 4, pp. 2611–2621, 2019.

[11] Z. Yang, P. Dehghanian, and M. Nazemi, "Enhancing seismic resilience of electric power distribution systems with mobile power sources," in *2019 IEEE Industry Applications Society Annual Meeting*, pp. 1–7, IEEE, 2019.

[12] S. Lei, C. Chen, Y. Li, and Y. Hou, "Resilient disaster recovery logistics of distribution systems: Co-optimize service restoration with repair crew and mobile power source dispatch," *IEEE Trans. on Smart Grid*, 2019.

[13] S. Lei, C. Chen, H. Zhou, and Y. Hou, "Routing and scheduling of mobile power sources for distribution system resilience enhancement," *IEEE Transactions on Smart Grid*, 2018.

[14] A. Asrari, S. Lotfifard, and M. Ansari, "Reconfiguration of smart distribution systems with time varying loads using parallel computing," *IEEE Transactions on Smart Grid*, vol. 7, no. 6, pp. 2713–2723, 2016.

[15] K. Sampath, S. Pattabiraman, M. Kannan, K. Narayanan, *et al.*, "Power loss minimization in radial distribution system through network reconfiguration," in *2019 IEEE 1st International Conference on Energy, Systems and Information Processing (ICESIP)*, pp. 1–5, IEEE, 2019.

[16] A. M. Imran, M. Kowsalya, and D. Kothari, "A novel integration technique for optimal network reconfiguration and distributed generation placement in power distribution networks," *International Journal of Electrical Power & Energy Systems*, vol. 63, pp. 461–472, 2014.

[17] S. Mishra, D. Das, and S. Paul, "A comprehensive review on power distribution network reconfiguration," *Energy Systems*, vol. 8, no. 2, pp. 227–284, 2017.

[18] M. Nazemi, P. Dehghanian, and M. Lejeune, "A mixed-integer distributionally robust chance-constrained model for optimal topology control in power grids with uncertain renewables," in *2019 IEEE Milan PowerTech*, pp. 1–6, IEEE, 2019.

[19] Z. Yang, P. Dehghanian, and M. Nazemi, "Seismic-resilient electric power distribution systems: Harnessing the mobility of power sources," *IEEE Transactions on Industry Applications*, vol. 56, no. 3, pp. 2304–2313, 2020.

[20] S. Iwai, T. Kono, M. Hashiwaki, and Y. Kawagoe, "Use of mobile engine generators as source of back-up power," in *31st IEEE International Telecommunications Energy Conference*, pp. 1–6, 2009.

[21] M. Lavorato, J. F. Franco, M. J. Rider, and R. Romero, "Imposing radiality constraints in distribution system optimization problems," *IEEE Transactions on Power Systems*, vol. 27, no. 1, pp. 172–180, 2012.

[22] M. E. Baran and F. F. Wu, "Network reconfiguration in distribution systems for loss reduction and load balancing," *IEEE Transactions on Power delivery*, vol. 4, no. 2, pp. 1401–1407, 1989.

[23] P. M. Castro, "Tightening piecewise mccormick relaxations for bilinear problems," *Computers & Chemical Eng.*, vol. 72, pp. 300–311, 2015.

[24] H. H. Abdeltawab and Y. A.-R. I. Mohamed, "Mobile energy storage scheduling and operation in active distribution systems," *IEEE Transactions on Industrial Electronics*, vol. 64, no. 9, pp. 6828–6840, 2017.

[25] S. Lei, J. Wang, C. Chen, and Y. Hou, "Mobile emergency generator pre-positioning and real-time allocation for resilient response to natural disasters," *IEEE Transactions on Smart Grid*, vol. 9, no. 3, pp. 2030–2041, 2016.

[26] H. Gao, Y. Chen, S. Mei, S. Huang, and Y. Xu, "Resilience-oriented pre-hurricane resource allocation in distribution systems considering electric buses," *Proceedings of the IEEE*, vol. 105, no. 7, pp. 1214–1233, 2017.

[27] G. Wang, X. Zhang, H. Wang, J.-C. Peng, H. Jiang, Y. Liu, C. Wu, Z. Xu, and W. Liu, "Robust planning of electric vehicle charging facilities with an advanced evaluation method," *IEEE Transactions on Industrial Informatics*, vol. 14, no. 3, pp. 866–876, 2017.

[28] O. K. Siirto, A. Safdarian, M. Lehtonen, and M. Fotuhi-Firuzabad, "Optimal distribution network automation considering earth fault events," *IEEE Transactions on Smart Grid*, vol. 6, no. 2, pp. 1010–1018, 2015.